



Cite this: *Dalton Trans.*, 2025, **54**, 2209

## Push–pull effect – how to effectively control photoinduced intramolecular charge transfer processes in rhenium(i) chromophores with ligands of D–A or D– $\pi$ –A structure†

Katarzyna Choroba, \* Joanna Palion-Gazda, Anna Kryczka, Ewa Malicka and Barbara Machura

Over the last five decades, diimine rhenium(i) tricarbonyl complexes have been extensively investigated due to their remarkable and widely tuned photophysical properties. These systems are regarded as attractive targets for design functional luminescent materials and performing fundamental studies of photoinduced processes in transition metal complexes. This review summarizes the latest developments concerning Re(i) tricarbonyl complexes bearing donor–acceptor (D–A) and donor– $\pi$ –acceptor (D– $\pi$ –A) ligands. Such compounds can be treated as bichromophoric systems with two close-lying excited states, metal-to-ligand charge transfer (MLCT) and intraligand-charge-transfer (ILCT). A role of ILCT transitions in controlling photobehaviour was discussed for Re(i) tricarbonyls with six different diimine cores decorated by various electron-rich amine, sulphur-based and  $\pi$ -conjugated aryl groups. It was evidenced that this approach is an effective tool for enhancement of the visible absorptivity, bathochromic emission shift and significant prolongation of the excited-state, opening up new possibilities in the development of more efficient materials and expand the range of their applications.

Received 19th November 2024,  
Accepted 2nd January 2025

DOI: 10.1039/d4dt03237c

rsc.li/dalton

## 1. Background and introduction

Since the pioneering work of Wrighton and Morse in the middle of the 1970s,<sup>1</sup> rhenium(i) tricarbonyl complexes with chelating  $\alpha$ -diimine ( $N^{\text{R}}N$ ) ligands have occupied a prominent position among photoluminescent molecular materials. The convenient and easy synthesis, thermal and photochemical stability, and outstanding photophysical behaviour make complexes  $[\text{ReL}(\text{CO})_3(\text{N}^{\text{R}}\text{N})]^n$  ( $\text{L}$  = ancillary ligand,  $n = 0$  or  $1+$ ) appealing for employment in optoelectronics,<sup>2–8</sup> photocatalysis<sup>9–18</sup> and life science.<sup>19–40</sup> The photophysical parameters of these systems, including the visible absorptivity, emission energy, quantum yield and triplet excited state lifetime, are adjusting to requirements of their potential applications by proper structural modifications of  $\alpha$ -diimine core and alteration of the ancillary ligand.

Along with promising functional features, Re(i) tricarbonyl complexes are perfectly suited for fundamental studies of photoinduced processes whose precise control is a key to success of designing compounds with pre-defined photo-

physical parameters. In this regard, the great advantage of  $[\text{ReL}(\text{CO})_3(\text{N}^{\text{R}}\text{N})]^n$  systems is the existence in the coordination sphere of the single diimine ligand, allowing to avoid the problem of excited-electron localization, and presence of carbonyl ligands, acting as efficient IR markers of redistribution of electron density upon photoexcitation. Excited-state dynamics of  $[\text{ReL}(\text{CO})_3(\text{N}^{\text{R}}\text{N})]^n$  have been widely investigated using ultrafast experimental methods like time-resolved infrared spectroscopy, fluorescence up-conversion methods, time-resolved emission spectroscopy and transient absorption.<sup>41–52</sup>

As demonstrated in ref. 53–60, the diverse photophysical behaviour of  $[\text{ReL}(\text{CO})_3(\text{N}^{\text{R}}\text{N})]^n$  is attributed to different triplet excited state nature metal-to-ligand charge transfer (MLCT), ligand-to-ligand charge transfer (LLCT), ligand-centered (IL), intraligand-charge-transfer (ILCT) nature or their superposition, controlled by the structural and electronic features of  $\alpha$ -diimine and ancillary ligands. The molecules in different excited states brings different emission characteristics.

In this article, we summarized the latest developments concerning Re(i) tricarbonyl complexes bearing donor–acceptor (D–A) and donor– $\pi$ –acceptor (D– $\pi$ –A) ligands. The attachment of the organic push–pull chromophore to the  $\{\text{Re}(\text{CO})_3\}^+$  core can results in new photophysical properties owing to the dominant role of ILCT transitions, with the charge flow from the electron-donating organic group (D) to the accepting diimine core (A).

Institute of Chemistry, Faculty of Science and Technology, University of Silesia, Szkolna 9, 40-006 Katowice, Poland.

E-mail: barbara.machura@us.edu.pl, katarzyna.choroba@us.edu.pl

† Electronic supplementary information (ESI) available. See DOI: <https://doi.org/10.1039/d4dt03237c>



The efficiency of intramolecular charge transfer in the coordinated D-A and D- $\pi$ -A ligands may be widely modified by the donor and acceptor strengths of electron-accepting and electron-donating components in the molecular diimine skeleton, their electronic coupling, as well as the environment – solvent polarity, hydrogen bonding with polar solvents.<sup>61–63</sup>

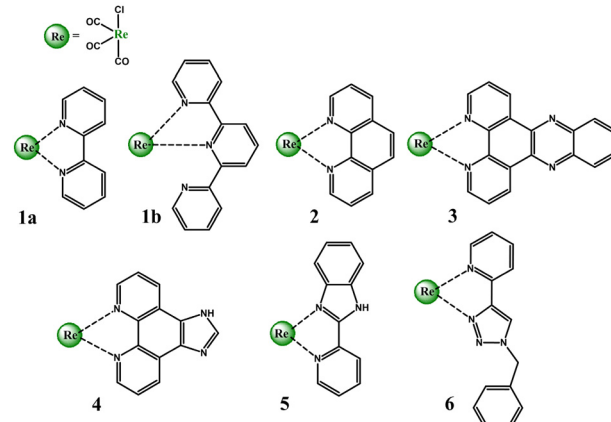
Regarding functional photophysical parameters of resulting complexes  $[\text{ReL}(\text{CO})_3(\text{N}^\wedge\text{N})]^\eta$ , the incorporation of D-A and D- $\pi$ -A into the coordination sphere of Re(i) tricarbonyl complexes may be an effective tool for enhancement of the visible absorptivity, bathochromic emission shift and significant prolongation of the excited-state. Photoactive red or NIR light emitting transition metal complexes with extended excited state lifetimes are strongly desirable for the photodynamic therapy (PDT),<sup>24,25,33,64,65</sup> time-resolved bioimaging,<sup>66</sup> and triplet-triplet annihilation up-conversion (TTA UC) techniques.<sup>67–69</sup> Understanding and precise controlling of long-lived charge-separated excited states in these systems still remains a major challenge and is crucial for designing improved functional materials.

To better illustrate the impact of the incorporated donor group on the photobehavior Re(i) carbonyl complexes, excited-state dynamics and photophysics of the most representative prototypical chromophores  $[\text{ReCl}(\text{CO})_3(\text{N}^\wedge\text{N})]$  with 2,2'-bipyridine (bipy), 1,10-phenanthroline (phen), dipyrido[3,2-*a*:2',3'-*c*]phenazine (dppz), imidazo[4,5-*f*][1,10]phenanthroline (imphen), 2-(2-pirydyl)benzimidazole (pybimd) and 2-(1-benzyl-1*H*-1,2,3-trizol-4-yl)pyridine (pytri-Bn) are firstly discussed. In the next sections, we concentrate on the optical properties and photoinduced processes of  $[\text{ReL}(\text{CO})_3(\text{N}^\wedge\text{N})]^\eta$  bearing these diimine  $\pi$ -acceptor ligands functionalized with electron-rich amine, sulphur-based and  $\pi$ -conjugated aryl groups. The final part presents the most appealing applications of Re(i) complexes with D-A or D- $\pi$ -A diimine ligands.

## 2. Prototypical Re(i) chromophores

Over five decades of intensive investigations, 2,2'-bipyridine (bipy), 1,10-phenanthroline (phen), dipyrido[3,2-*a*:2',3'-*c*]phenazine (dppz), imidazo[4,5-*f*][1,10]phenanthroline (imphen), 2-(2-pirydyl)benzimidazole (pybimd) and 2-(1-benzyl-1*H*-1,2,3-trizol-4-yl)pyridine (pytri-Bn) and their derivatives have become the most recognizable and most extensively studied diimine ligands in the Re(i) coordination chemistry. As 2,2':6',2"-terpyridine (terpy) may coordinate to the metal center of the  $\{\text{Re}(\text{CO})_3\}^+$  core in a bidentate mode and form  $[\text{ReL}(\text{CO})_3(\text{terpy}-\kappa^2\text{N})]^\eta$  systems analogous to that with bipy, it has also been taken into considerations in this section (Scheme 1).

Possessing low lying  $\pi^*$  orbitals, bipy, terpy, phen, dppz, imphen, pybimd and pytri-Bn act as  $\pi$ -acceptor ligands upon attachment to the electron-rich  $\{\text{Re}(\text{CO})_3\}^+$  core. For all complexes,  $[\text{ReCl}(\text{CO})_3(\text{bipy})]$  (**1a**),  $[\text{ReCl}(\text{CO})_3(\text{terpy}-\kappa^2\text{N})]$  (**1b**) [ $[\text{ReCl}(\text{CO})_3(\text{phen})]$  (**2**),  $[\text{ReCl}(\text{CO})_3(\text{dppz})]$  (**3**),  $[\text{ReCl}(\text{CO})_3(\text{imphen})]$  (**4**),  $[\text{ReCl}(\text{CO})_3(\text{pybimd})]$  (**5**) and  $[\text{ReCl}(\text{CO})_3(\text{pytri-Bn})]$  (**6**)<sup>70</sup>, the LUMO resides on the diimine core, while the HOMO, H-1 and



Scheme 1 Re(i) tricarbonyl complexes discussed in this section.

H-2 are contributed by  $d_\pi$  rhenium orbitals in a bonding relation to the carbonyl  $\pi^*$  orbitals and an antibonding arrangement to the chlorine occupied p orbitals (Fig. 1). Regarding the LUMO distribution, a more detailed comment is required for Re(i) complexes **1b**, **3**, **4** and **6**. The LUMO of **1b** is delocalized over the two coordinated rings – the bipy-like moiety, as in **1a**. In the case of **3** bearing dppz, which can be considered as a fusion of phenanthroline (phen) and phenazine (phz), the DFT calculations indicate a predominant contribution of the phz component in the lowest unoccupied molecular orbital. The phenanthroline  $\pi$ -antibonding orbitals participate in the higher lying LUMO+1. The LUMO of **4** is solely contributed by the phen core, while the higher in energy LUMO+1 is delocalized over the whole imphen ligand. As the triazole ring acts as an electronic insulator,<sup>70</sup> the benzyl (Bn) molecular orbitals show no contribution in LUMO of **6**, signalling that substituents introduced in this part of the pytri ligand have negligible impact on optical properties (Fig. S1 and S2†). As demonstrated in Fig. 1, the HOMO-LUMO gap of **1a**, **1b**, **2**, **4** and **5** varies in a small range 3.88–3.91 eV. The introduction of dppz into the Re(i) coordination sphere results in a noticeable decrease in the HOMO-LUMO gap (3.51 eV), contrary to pytri-Bn which induces its increase (4.32 eV).

Theoretically assigned character of the frontier molecular orbitals of **1–6** was fully supported by electrochemical studies. For all complexes **1–6**, the first oxidation wave is associated with the oxidation of metal centre Re(i/ii), while the reduction occurs in the diimine core (Table S1†). For complex **3**, the reduction potential is much closer to that of phz than that of bipy or phen, supporting the involvement of phz MO orbitals in the reduction process.<sup>71</sup>

Based on the frontier molecular energy diagram, an electron can be promoted from the  $d_\pi(\text{Re})$  into  $\pi^*$  diamine orbitals, giving rise to MLCT transitions, which determine the optical properties of these systems. For complex **3**, the lowest singlet excited state is of  $\text{MLCT}_{\text{phz}}$  nature.<sup>44,72,73</sup> Due to participation of the halogen orbitals in the highest occupied molecular orbitals, the first excited state of **1–6** may also be classified as

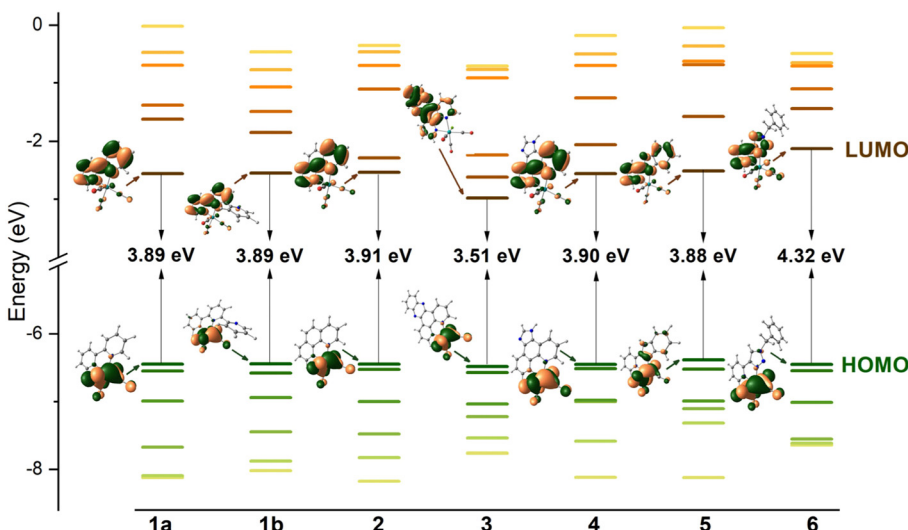


**Fig. 1** Frontier molecular orbitals energy diagram for complexes **1–6** along with electron density plots of the highest occupied and lowest unoccupied MOs.

MLLCT (metal-ligand-to-ligand charge transfer). However, regarding that MLCT predominates over XLCT in chloride diamine  $\text{Re}(\text{i})$  tricarbonyls,<sup>41,46,74</sup> the simplified notation is used in this article.

All complexes **1–6** are characterized by the weak absorptivity in the region 320–400 nm covering  $^1\text{MLCT}$  spin-allowed transitions (Table S2†). The reason of their weak absorptivity is the poor spatial overlap of HOMOs contributed by  $d_{\pi}$  metal orbitals and LUMO localized on  $\pi^*$  diimine molecular orbitals. In most cases, the MLCT absorption lies at low energy edge of the intense band attributed to  $\pi-\pi^*$  intraligand (IL) transitions.

As demonstrated by fluorescence up-conversion (FLUC), UV-Vis transient absorption (TA), or time-resolved infrared (TRIR) spectroscopies,<sup>43,45,47,50–52,75,76</sup> the optically populated  $^1\text{MLCT}$  state of **1a**, **1b**, **2** and **4** undergoes the efficient intersystem crossing (ISC) in tens of femtoseconds, populating an interligand-localized excited state ( $^3\text{IL}$ ) and vibrationally hot  $^3\text{MLCT}$  excited states. On a picosecond timescale, depending on the solvent and ancillary ligand,  $^3\text{IL}$  is converted into the  $^3\text{MLCT}$  excited state. The vibrationally relaxed  $^3\text{MLCT}$  state decays then to the ground state. TA spectra of these systems are characterized by intense band in the near UV region due to  $\pi-\pi^*$  transitions localized at the formally reduced diimine ligand and the broad excited state absorption (ESA) across the entire visible region (400–650 nm) originating from  $\text{Cl}/\text{diamine}^{\cdot-} \rightarrow \text{Re}$  (ligand-to-metal charge-transfer, LMCT) triplet-triplet transitions. Consistent with the removal of electron density from the  $\pi^*$  antibonding orbital of the carbonyl groups after the MLCT photoexcitation, the TRIR spectra of **1a** and **2** show a shift of  $\nu_{\text{CO}}$  to higher energies, with the magnitude of the positive  $\nu_{\text{CO}}$  band shifts of  $40\text{--}60\text{ cm}^{-1}$ .<sup>41,57,77</sup> For complexes **5** and **6**, the formation of  $^3\text{MLCT}$  excited state was postulated on the basis of steady-state and time-resolved spectroscopic data accompanied with theoretical calculations, as

well as more advanced techniques for related systems.<sup>70,78–83</sup> Using the TRIR technique,  $^3\text{MLCT}$  character was evidenced for the bromide analogue of the complex **6**.<sup>70</sup>

The introduction of the dppz ligand into the  $\text{Re}(\text{i})$  coordination sphere resulted in a greater triplet excited state diversity, as a result of possessing of close-lying MLCT and IL excited states.<sup>44,50</sup> The excited state dynamics of **3** in solvents of different polarity was explored by TRIR spectroscopy. The photophysics of this complex in polar  $\text{MeCN}$  and  $\text{C}_3\text{H}_7\text{CN}$  was found to be governed by  $^3\text{MLCT}_{\text{phz}}$ ,  $^3\text{MLCT}_{\text{phen}}$  and  $^3\text{IL}_{\pi-\pi^*}$  excited states, while the formation of only  $^3\text{MLCT}_{\text{phen}}$  and  $^3\text{IL}_{\pi-\pi^*}$  was revealed in non-polar  $\text{CH}_2\text{Cl}_2$ . The increased solvent polarity was evidenced to lead to a higher population of  $^3\text{MLCT}_{\text{phz}}$  excited state. Contrary to  $^3\text{MLCT}_{\text{phen}}$ ,  $^3\text{MLCT}_{\text{phz}}$  excited state is dark. In general, two sets of transient bands are observed in TRIR spectra of **3**, that are shifted to higher and lower energy relative to the parent  $\nu_{\text{CO}}$  absorptions, respectively. The former ones are characteristic of the  $^3\text{MLCT}$  excited state, while those with negative shifts represent  $^3\text{IL}_{\pi-\pi^*}$ . The difference between  $^3\text{MLCT}_{\text{phz}}$ ,  $^3\text{MLCT}_{\text{phen}}$  concerns the magnitude of the positive shift. The phz-based MLCT excited state are represented by  $\nu_{\text{CO}}$  transient absorptions shifted to higher wavenumber in comparison to those of  $^3\text{MLCT}_{\text{phen}}$ .<sup>44,50</sup>

Typically of  $^3\text{MLCT}$  emitters, the emission spectra of **1a**, **1b**, **2**, **4** exhibit broad and unstructured band in both solution and rigid-glass matrix (77 K). Consistent with the rigidochromic effect, the frozen-state emission bands of these systems are noticeably blue-shifted and show extended lifetime relative to those at room temperature.<sup>52,84,85</sup> The emission properties of **5** and **6** were largely studied only in solution at RT, and broad structureless  $^3\text{MLCT}$  emission band was evidenced for both of them.<sup>80–82,86–88</sup> The complex **3** was found to possess more complicated emission features due to an interplay between two, close in energy,  $^3\text{MLCT}$  and  $^3\text{IL}$  excited states. At tempera-

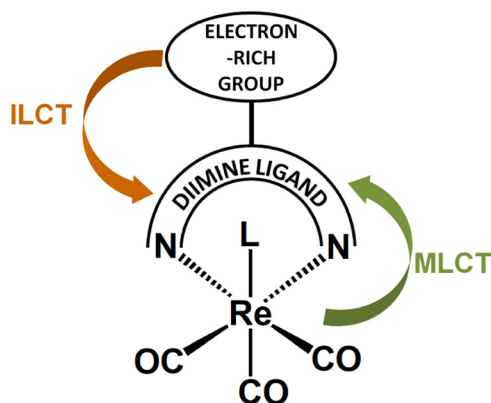


ture  $>145$  K, the complex **3** behaves as  $^3$ MLCT emitter, showing unstructured emission band. With decreasing temperature, it becomes a  $\pi-\pi^*$  emitter, with long lifetime and structured profile of the emission band.<sup>72,89</sup> The wavelength emission maxima of **1–6** in solutions at RT generally cover the yellow-orange spectral region. The triplet state lifetimes of these systems, albeit noticeably longer than fluorescence lifetimes of organic chromophores, are usually shorter than 500 ns (Table S2<sup>†</sup>), which is rationalized by the fact that the metal parentage in a triplet excited state increases the radiative decay rate constant. The excited-state lifetimes of **1–6** are usually insufficiently long enough for efficient intermolecular photo-induced energy- or electron-transfer processes, required for such applications as photodynamic therapy, time-resolved bio-imaging, or triplet-triplet annihilation up-conversion. Regarding above-mentioned applications, also the weak visible absorptivity of **1–6** is a significant disadvantage.

### 3. Rhenium(i) chromophores with D–A or D– $\pi$ –A diimine ligands

Functionalization of diimines with electron-rich donors leads to the increase in the level of complexity in the photophysical behavior of complexes  $[\text{ReL}(\text{CO})_3(\text{N}^{\text{+}}\text{N})]^n$ . In such systems, two distinct photoinduced charge flow processes are possible, that are from the peripheral donor substituents to the diimine core, and from metal center to the  $\pi$ -acceptor diimine framework, as illustrated in Scheme 2. Such systems can be regarded as bichromophoric systems with two close in energy MLCT and ILCT states.

The interplay between MLCT and ILCT excited states, as well as perturbations in photophysics of  $[\text{ReL}(\text{CO})_3(\text{N}^{\text{+}}\text{N})]^n$  due to the ILCT involvement are discussed below for Re(i) bearing the diimine  $\pi$ -acceptor framework functionalized with the amine, sulphur-based and  $\pi$ -conjugated aryl groups, regarded as most recognizable and most extensively studied donors.



**Scheme 2** Schematic structure of the Re(i) carbonyl chromophore with D–A diimine ligand, along with two possible photoinduced charge flow processes.

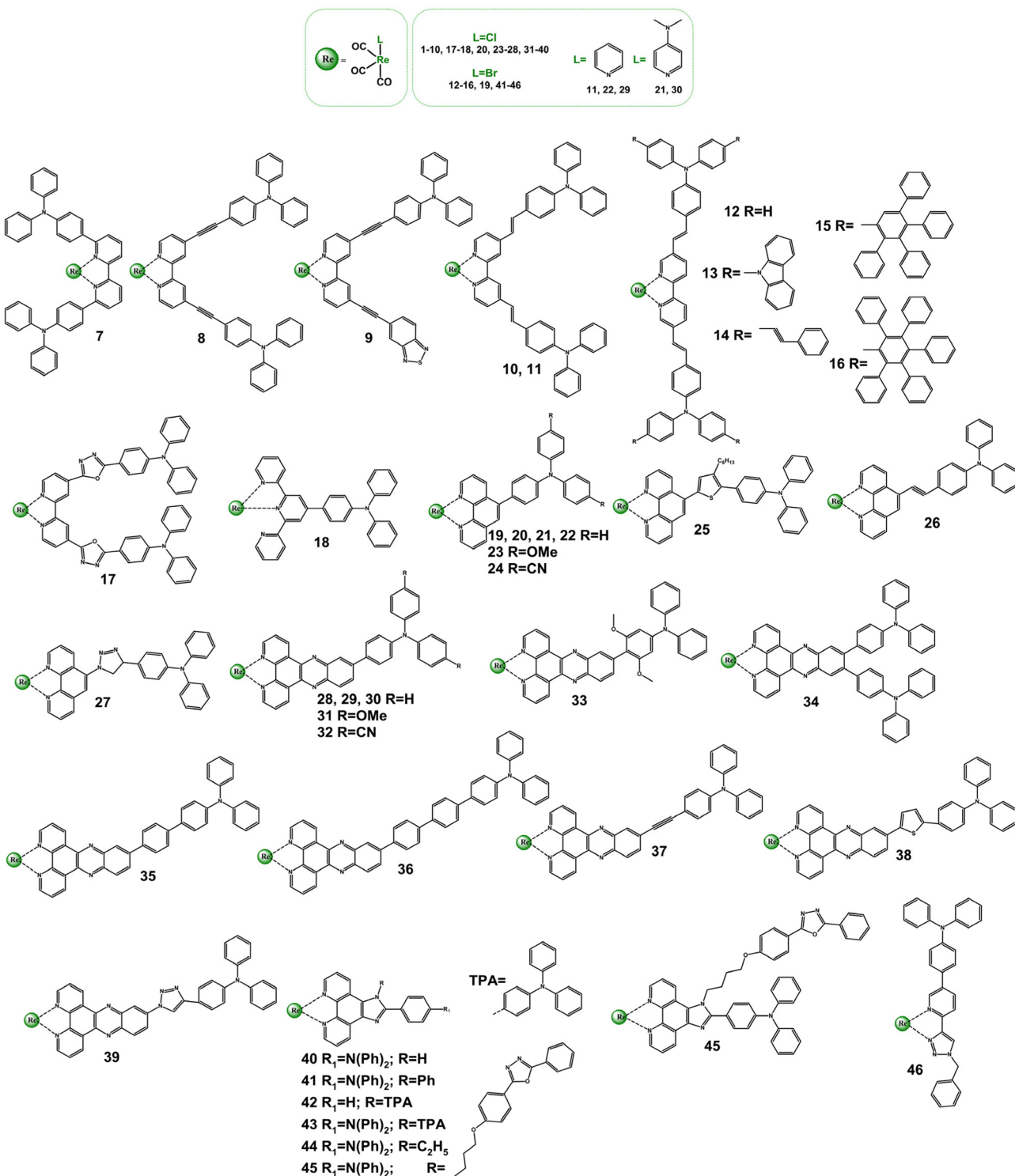
#### 3.1. Amine-substituted ligands

Extensive research has been done to study ground and excited states of Re(i) complexes with diimine ligands functionalized with strong electron-donating triphenylamine (TPA) group, demonstrated in Scheme 3 and Table S3.<sup>†</sup><sup>5,52,70,90–105</sup> Investigations in this field were largely performed by Gordon's research group with the use of a wide spectrum of spectroscopic techniques, including transient absorption and emission, time-resolved IR and Raman spectroscopies.<sup>70,93,95–100,102–105</sup>

The structural modification of bipy with TPA motive leads to noticeably perturbations in the photophysics of all complexes **7–16** relative to the parent chromophore **1**. However, only for systems **12–16**, ILCT excited states become dominated in controlling their photobehaviour. Consistent with the contribution of  $^1$ ILCT transitions, the lowest absorption band of these systems shows a bathochromic shift and experiences a large increase in the molar absorptivity compared to the reference chromophore **1**. The decreased contribution of  $^1$ ILCT transitions in the lowest energy absorption was indicated for **7** and **9**, which was rationalized by the large TPA–bipy dihedral angle for **7** and replacement of one of TPA groups by electron-withdrawing benzothiadiazole for **9**.<sup>103,104</sup>

The complexes **7–9** show dual fluorescence–phosphorescence emission, relatively rare observed for diamine Re(i) carbonyl complexes.<sup>103,104</sup> The lowest triplet emitting state of **7**, represented by the low energy component in the emission spectrum, was confirmed to possess  $^3$ MLCT nature. The energy and lifetime of the phosphorescence band of **7** is only slightly lower than those for the parent chromophore **1**.<sup>103</sup> The relative intensities of the fluorescence–phosphorescence components of **8** and **9** were found to be strongly dependent on the polarity environment, showing a significant drop in triplet emission intensities in more polar solvents. Gordon's research group evidenced that triplet excited states of these systems vary in nature, depending on the solvent polarity. In less polar  $\text{CH}_2\text{Cl}_2$ , the emissive state is of  $^3$ MLCT nature. In polar MeCN, the lowest triplet state is of  $^3$ ILCT character. It is a dark state, populated *via* internal conversion from  $^3$ MLCT<sup>104</sup> (Fig. 2).

The variable contribution of  $^3$ ILCT in the lowest triplet state depending on the solvent polarity was also postulated for **18**.<sup>101</sup> The complexes **10** and **11** show the single emission band, with maximum at  $\sim 520$  nm and lifetime shorter than 10 ns, assigned to prompt fluorescence from  $^1\pi \rightarrow \pi^*$  state. In similarity to **8** and **9** in polar environment, the lowest triplet state of **10** and **11** is dark, but its character was assigned as a mixed  $^3$ ILCT and  $^3$ IL. The  $^3$ IL contribution was rationalized by the large overlapping of the donor and acceptor orbitals. Compared to **8** in MeCN, the complex **10** shows a noticeably elongated lifetime, 140 ns for **8** and 600 ns for **10**.<sup>93</sup> Outstanding emissive properties were revealed for **12–16**. All these systems exhibit broad unstructured emission band in a deep red to near-infrared range (680–708 nm), red-shifted with the increasing  $\pi$ -conjugation of the TPA unit, and originated from  $^3$ ILCT excited state. Importantly, the luminescence quantum yields of the systems with bulky amine groups (**15**



**Scheme 3** Re(i) carbonyl complexes bearing diimine ligands functionalized with the triphenylamine (TPA) motive.

and **16**) were found to be comparable to that of the non-substituted **12**, despite their red shift in emission energies.<sup>94</sup> The introduction of the oxadiazole linkage between bipy and TPA units resulted in the formation of Re(i) carbonyl complex (**17**) with the emitting state of  $^3\text{MLCT}$  nature, which was clearly evidenced by transient DC photoconductivity technique.<sup>90</sup>

In a series of Re(i) complexes bearing 1,10-phenanthroline with appended TPA donor group at the 5 position, the relative energies and ordering of MLCT and ILCT charge transfer excited states were tuned by (i) changing the electron withdrawing ability of the ancillary ligand (**19-22**), (ii) modulating the donating ability of the TPA group through the introduction

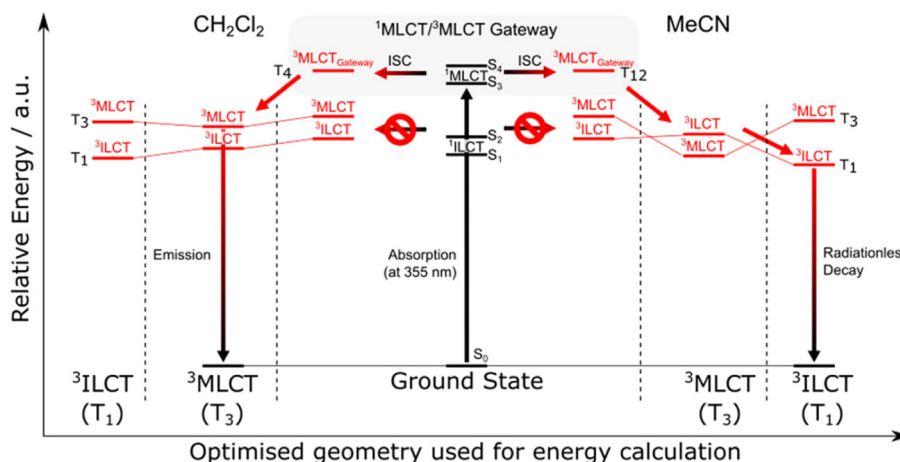


Fig. 2 Relative energies of excited states and transitions for **8** in  $\text{CH}_2\text{Cl}_2$  and MeCN. Reprinted with permission from ref. 104 Copyright © 2021, American Chemical Society.

of additional methoxy and cyano groups (23 and 24), (iii) using various bridging groups between the TPA and diimine units (25–27).<sup>99,102,105</sup>

Independent on the electron withdrawing ability of the ancillary ligand, for all four complexes **19–22**, the lowest-energy absorption region is dominated by  $^1\text{ILCT}$  transitions, and the emissive excited state remains  $^3\text{ILCT}$ . All these systems are characterized by strong visible absorptivity, red shifted with increasing the electron withdrawing ability of the ancillary ligand. Outstanding emissive photophysical properties were revealed for the halide species **19** and **20**. Their excited-state lifetimes (6  $\mu\text{s}$  for **19** and 3.9  $\mu\text{s}$  for **20**) were found to be longer by 2 orders of magnitude in relation to the non-halide systems (44 ns for **21** and 27 ns **22**) and parent chromophore **2** (Table S2†). To explore different behaviour of the halide complexes (**19** and **20**) to non-halide ones (**21** and **22**), transient absorption and emission, transient resonance Raman, and time-resolved infra-red spectroscopy in combination with TD-DFT calculations were utilized. The complexes **19** and **20** were found to possess spectral signatures from both  $^3\text{MLCT}$  and  $^3\text{ILCT}$  states, contrary to the non-halide systems with contribution of only  $^3\text{ILCT}$ . The impact of the ancillary ligand on the excited state lifetimes of **19–22** was explained in terms of energy-gap law.<sup>99</sup> The introduction of additional electron-donating methoxy groups into TPA moiety leads to the stabilization of the  $^3\text{ILCT}$  state in **23** compared to **20**, but complex **23** becomes non-emissive in solution at RT, in contrast to **20**. Typically of Re(i) systems with diimine ligands functionalized with the TPA group, TA spectra of **23** show an excited-state absorptions consistent with  $\text{TPA}^+$  (750–800 nm) and  $\text{phen}^-$  (330–390 nm). The excited-state lifetime of  $^3\text{ILCT}$ , obtained from transient absorption measurements of **23** (28 ns), was found to be shorter by 2 orders relative to that of **20** (3.9  $\mu\text{s}$ ). For complex **24** with additional electron-withdrawing cyano groups in TPA motive, the  $^3\text{ILCT}$  excited states is noticeably destabilized in comparison to that of **20**, becoming near-is-

energetic with  $^3\text{MLCT}$  excited state. Competitive excited-state relaxation pathways with contribution of  $^3\text{ILCT}$  and  $^3\text{MLCT}$  was postulated for **24**. The complex emits at  $\sim$ 600 nm at RT, and shows a relatively long excited-state lifetime (290 ns).<sup>102</sup> The incorporation of an electronically conducting linker (thiophene-based in **25** and ethynyl unit in **26**) was found to facilitate the TPA–phen communication, leading to the formation of  $^3\text{ILCT} / ^3\text{IL}$  dark excited states with long biexponential lifetimes, up to 45  $\mu\text{s}$ . Such long-lived excited states were firstly confirmed for transition metal complexes with phen-TPA derivatives. Contrastingly, the 1,2,3-triazole bridge, a well-known electronic insulator, disrupts the TPA–phen communication in **27**. Unlike **25** and **26**, the complex **27** exhibits weak emission at  $\sim$ 600 nm, with excited-state lifetime of 60 ns. The lowest triplet state of **27** was postulated to be  $^3\text{MLCT}$  in nature.<sup>105</sup>

The impact of the ancillary ligand, additional groups in the TPA motive and D–A linkers on the interplay between MLCT and ILCT was also widely explored for Re(i) carbonyl complexes with TPA-appended dppz ligands (**28–39**). As reported in a previous section, the photophysics of Re(i) systems with dppz-based ligand may be more complex compared to complexes with other diimine ligands, owing to the presence of close-lying  $\text{MLCT}_{\text{phen}}$ ,  $\text{MLCT}_{\text{phz}}$  and IL excited states.

The Frank-Condon photophysics of all systems **28–39** was found to be predominately contributed by  $^1\text{ILCT}$  transitions. The introduction of additional electron-donating groups into TPA motive and replacement of the halide ancillary ligand by pyridine or dimethylaminopyridine result in a bathochromic shift of the broad intense ILCT band relative to **28**. Contrastingly, the extended donor–acceptor distance induces a blue-shift of the ILCT absorption, while the increased D–A torsion angle, leading to the poorer overlap of the donor and acceptor molecular orbitals, is manifested by a noticeably drop in molar absorptivity of the ILCT band. Excited-state photophysics of all complexes **28–39** is also controlled by ILCT



states.<sup>95–98,100</sup> The compounds **28–30** were evidenced to exhibit a weak emission, originating from the triplet state of ILCT character and showing a linear correlation between the Stokes shift and solvent polarity. All these systems are characterised by the increase in the emission intensity with increasing temperature, indicated the thermal equilibrium with a dark triplet excited state of lower energy. By TRIR spectroscopy, this dark state was assigned as phz-based <sup>3</sup>ILCT, with lifetimes from 1.4 to 10.1  $\mu$ s.<sup>95</sup> The incorporation of additional groups into the TPA motive results in formation of complexes, which show fluorescence occurring from <sup>1</sup>ILCT excited state, strongly dependent on the substituent and solvent polarity (31 and 32). Contrastingly, the lifetimes of the lowest triplet dark states <sup>3</sup>ILCT of **31** and **32**, confirmed through TA spectroscopy, are only slightly affected by the appended substituents: 3.8  $\mu$ s for **28**, 3.6  $\mu$ s for **31** and 3.0  $\mu$ s for **32**.<sup>97</sup> The excited-state photo-physics of other Re(i) with dppz-based ligand (**33–39**) is also governed by <sup>3</sup>ILCT state, populated from <sup>1</sup>ILCT. However, variations in the donor–acceptor communication, achieved by the modulation of D–A torsion angle, D–A distance and linker nature, lead to changes of <sup>3</sup>ILCT lifetimes, which range from 3.9  $\mu$ s for **34** to 600 ns for **39**.<sup>98,100</sup> All complexes **33–39** show short-lived emission (<6 ns).

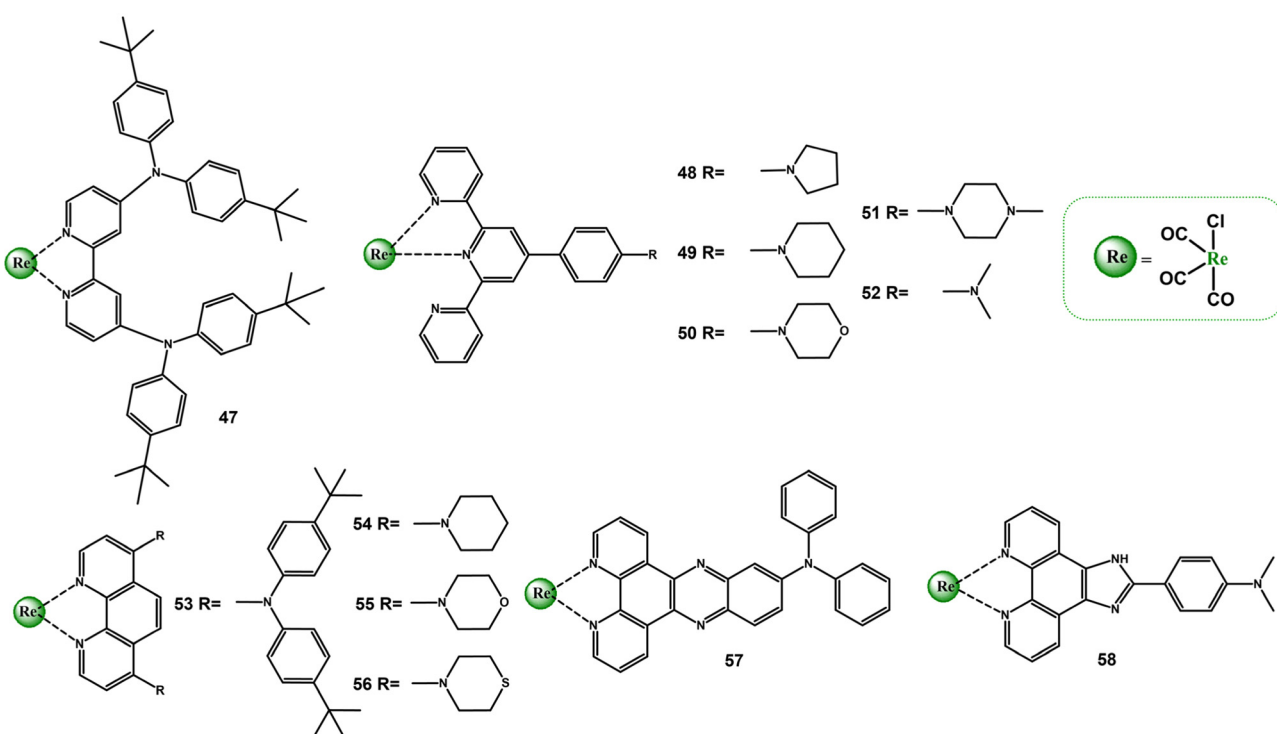
So far, little attention has been paid to Re(i) complexes with TPA-appended imphen ligands. The photophysics of **40–45** has been not explored with the use of transient absorption and emission, time-resolved IR and Raman spectroscopies. The attachment of TPA does not result in an efficient improvement of the visible-light absorptivity of **40–45**. The relatively weak lowest energy absorption of **40–45**, tailing up to 500 nm, was

tentatively assigned to <sup>1</sup>MLCT excited state. All these systems exhibit phosphorescence at ~600 nm, tentatively attributed to <sup>3</sup>MLCT admixed with <sup>3</sup>IL/ <sup>3</sup>ILCT. Regarding good photophysical functional parameters (quantum yields and excited-state lifetimes), excited-state dynamics in these systems deserves more scientific interest, especially that some of these compounds are efficient emitters in electrophosphorescent devices.<sup>5,52,91,92</sup>

As mentioned in the previous section, substituents appended to the triazole ring have a limited impact on photo-behaviour of Re(i) complexes bearing pytri-based ligands. On the contrary, the incorporation of TPA on the triazole ring of the pytri-Bn ligand has been proven to be a good way of controlling the ground and excited properties of this type of complexes. The TPA donor group efficiently improves the visible absorptivity of **46**, consistent with an involvement of <sup>1</sup>ILCT transitions in the lowest energy absorption. The complex **46** shows emission at 573 nm, red-shifted compared to the unsubstituted chromophore (549 nm) and most likely occurring from <sup>1</sup>ILCT excited state ( $\tau < 10$  ns). The TA and TRIR results are consistent with the formation of the <sup>3</sup>ILCT dark excited state, with a lifetime of 2.7  $\mu$ s.<sup>70</sup>

There have been several other interesting reports on the impact of other cyclic and acyclic amine substituents on the photophysics of diimine Re(i) carbonyl complexes (Scheme 4 and Table S4†).

A comparative analysis of photophysical properties of complexes **47**, **53** and **57** confirms a crucial role of the diimine core in controlling photobehaviour of Re(i) carbonyl complexes. Contrary to complexes **47** and **53**, which possess absorption and emission spectral features from both MLCT and IL/ILCT



Scheme 4 Re(i) carbonyl complexes bearing diimine ligands substituted with different types of amines.



states, affected additionally by the polarity environment, the singlet and triplet excited states of **57** are in predominately ILCT nature. Worthy of note, the intense visible absorption of **57** is bathochromically shifted compared to the complex with TPA motive (**28**), and its triplet excited-state lifetime is two times longer than that of **28**.<sup>100,106</sup> Outstanding absorption and emission properties were revealed for the complex **52**. The attachment of  $-NMe_2$  resulted in an appearance of a very intense visible absorption band and dramatic elongation of the emissive triplet excited state lifetime. Compared to the reference chromophore [ReCl(CO)<sub>3</sub>(Ph-terpy- $\kappa^2$ N)], the lowest energy absorption band is red-shifted by  $\sim$ 100 nm, and the triplet excited-state lifetime is 260 times longer. These distinct absorption and emission properties of **52** were assigned to <sup>1</sup>ILCT and <sup>3</sup>ILCT excited states, supported by TA and TRIR spectroscopies in accompany with TD-DFT calculations.<sup>107–109</sup> In turn, the introduction of  $-NMe_2$  group into the Ph-imphen does not result in the switch from <sup>3</sup>MLCT to <sup>3</sup>ILCT in **59**. The lowest energy absorption state of **59** is predominantly MLCT in nature, and its emission in non-polar solvents occurs from the triplet excited state of the mixed IL/ILCT/MLCT nature. The <sup>3</sup>IL/<sup>3</sup>ILCT character of the emitting triplet state is manifested by the red-shift of the emission band and increase in the lifetime relative to the reference chromophore [ReCl(CO)<sub>3</sub>(Ph-imphen)], as well as an appearance of the vibronic progression in frozen emission spectra profile of **59**.<sup>52</sup>

The photoluminescence properties of Re(i) complexes with Ph-terpy decorated with cyclic amines (**48–51**) were found to be strongly dependent on the polarity environment. It was evidenced that polar solvents facilitate the formation of <sup>3</sup>ILCT state, showing elongated lifetime relative to that of the model chromophore. The triplet excited state <sup>3</sup>ILCT of **48** was found to be sufficiently long for singlet oxygen generation.<sup>101,109–111</sup> The absorption and emission properties of Re(i) complexes with 1,10-phenanthroline decorated with piperidine (**54**), morpholine (**55**) and thiomorpholine (**56**) were attributed to configurationally mixed MLCT/IL excited states. The inclusion of cyclic amine groups into the phen core was found to be effective at improving molar absorptivity and extending excited-state lifetimes. The most pronounced increase in the lifetime was confirmed for **56** in CHCl<sub>3</sub> (6.67  $\mu$ s).<sup>85</sup>

### 3.2. Diimines with sulphur-based donor groups

The interplay between MLCT and ILCT charge processes in Re(i) tricarbonyl complexes with diimines bearing sulphur-based donor groups has received relatively little scientific attention so far. More detailed spectroscopic investigations were performed for only a few systems (Scheme 5 and Table S5†), mainly tetrathiafulvalene-, thiophene/oligothiophene- and phenothiazine-substituted diimine Re(i) carbonyl complexes.<sup>71,85,112–118</sup>

Except for **61**, the absorption and emission behaviour of thiophene-substituted Re(i) species (**59**, **64**) is dominated by MLCT/LLCT excited states.<sup>113,114</sup> The lowest energy singlet-singlet electronic transition of **61** was found to be ILCT in nature.<sup>115</sup> Independent on the diimine core, a degree of ILCT

character in the excited states of Re(i) complexes increases when the number of appended thiophene units becomes greater. An extension of the donor  $\pi$ -conjugation, promoting the charge-separated excited states in **60**, **62**, **63**, **65** and **66**, results in their noticeably red-shift and enhanced light absorption in the visible light range compared to corresponding thiophene-substituted or parent Re(i) systems.<sup>114,115,117,118</sup> The emission of **61–63** was shown to occur from <sup>1</sup>ILCT absorbing state. In agreement with TA studies and triplet state DFT calculations, the dark <sup>3</sup>ILCT/<sup>3</sup>IL triplet excited state of **61–63** is the result of a  $^1n,\pi \rightarrow ^3\pi,\pi$  transition, and the increased number in thiophene units induces higher contribution of <sup>3</sup>IL character in the excited state.<sup>115</sup> The TA spectra of **66** were found to possess signatures of either <sup>3</sup>MLCT and <sup>3</sup>ILCT/<sup>3</sup>IL excited states, and the <sup>3</sup>ILCT/<sup>3</sup>IL was postulated to participate in intermolecular charge transfer process between **66** and oxygen or biomolecules to generate reactive oxygen species (ROS).<sup>117</sup>

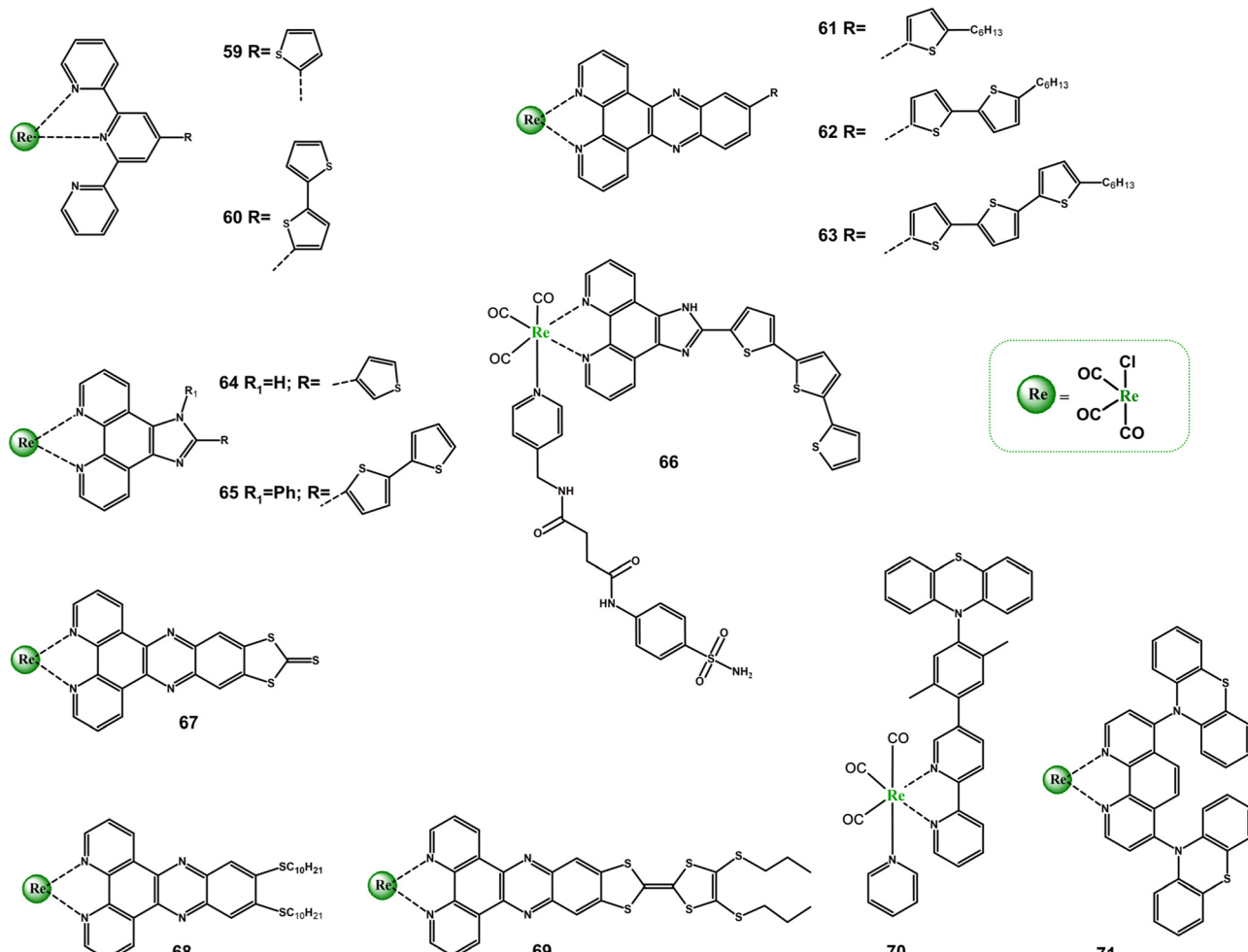
For complexes **67** and **68**, the absorption properties were analysed using TD-DFT calculations and resonance Raman spectroscopy, which confirm the occurrence of both MLCT and ILCT transitions.<sup>71</sup> A spectacular photobehaviour was revealed for the compound **69** possessing the lowest energy <sup>1</sup>ILCT absorption ( $\lambda_{max} = 580$  nm) well-separated from the higher lying <sup>1</sup>MLCT band ( $\lambda_{max} = 375$  nm). The direction of photo-induced charge-transfer processes in **69** can be controlled by the excitation wavelength. The excitation of **69** at 560 nm results in formation of the charge-separated state ILCT, representing by ESA of radicals TTF<sup>+</sup> and dppz<sup>–</sup>, decaying in the tens of ps regime, typically of TTF-based D–A systems. In turn, fs-TA spectra recorded upon 400 nm excitation exhibit features of both ILCT and MLCT transitions, with the predominant contribution of the latter ones. After 80 ps, only <sup>3</sup>MLCT is observed. The long-lived <sup>3</sup>MLCT was found to form via intersystem crossing <sup>1</sup>MLCT  $\rightarrow$  <sup>3</sup>MLCT.<sup>116</sup>

Regarding the phenothiazine-substituted systems (**70** and **71**), the formation of the charge separated excited state was directly evidenced only for **71**. The excited-state absorptions corresponding to the phenanthroline radical anion phen<sup>–</sup> (340 nm) and phenothiazine radical cation ptz<sup>+</sup> (530) were observed in TA spectra of **71** immediately after its laser excitation. On contrary, efforts to detect ptz<sup>+</sup> in **70** were failed. It was postulated that the photoinduced charge separation process is significantly slower than the thermal charge recombination in this system. Importantly, the complex **71** was found to be a rare example of NIR light-emitting system (785 nm in CHCl<sub>3</sub> with  $\tau = 150$  ns).<sup>85,112</sup>

### 3.3. ILCT contribution in Re(i) carbonyl complexes with diimines bearing $\pi$ -conjugated aryl groups

The incorporation of  $\pi$ -conjugated aryl groups into the diimine cores facilitates a population of the triplet ligand-centered excited state. When <sup>3</sup>MLCT and <sup>3</sup>IL states sharing similar energy, an excited state equilibrium is established, meaning that the organic chromophore repopulates the luminescent <sup>3</sup>MLCT excited state and may play a role of the energy “reservoir” or excited-state storage element. Such compounds are





**Scheme 5** Re(i) carbonyl complexes bearing diimine ligands substituted with sulphur-based donor groups.

generally emissive and show significantly extended excited state lifetimes in solution at RT. The prolonged lifetimes are also expected when the triplet excited state localized on the organic chromophore lies significantly lower in energy than  $^3\text{MLCT}$ , but these bichromophore systems are usually non-emissive in solution at RT.<sup>119–124</sup> The room-temperature phosphorescence attributable to the triplet excited state of  $\pi$ -conjugated aryl chromophore is extremely rarely observed.<sup>125–128</sup> The chromophoric units (organic and inorganic) maintains independent when they are perpendicularly arranged and the mixing of orbitals of both chromophores is minimized. Reducing the dihedral angle between the substituent and core of the organic ligand results in partial “mixing” of orbitals of both chromophores, and may lead to a noticeable contribution of ILCT excited states in the photobehaviour of resulting chromophore systems as  $\pi$ -conjugated aryl groups have potential to act as electron-donating substituents due to the high  $\pi$ -electron density.

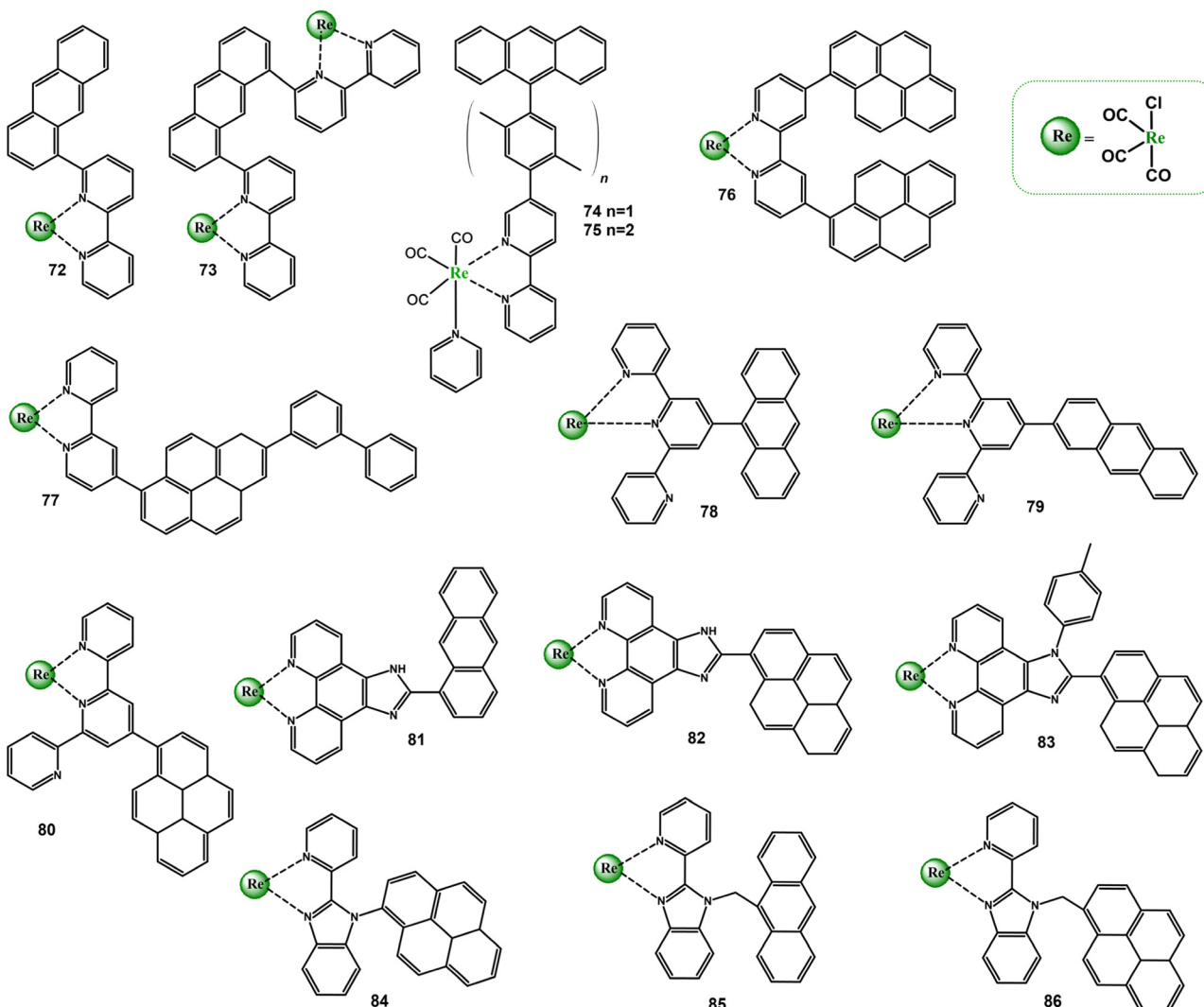
Among Re(i) complexes with diimine ligands substituted with electron rich  $\pi$ -conjugated aryl groups 72–86, demon-

strated in Scheme 6, a noticeable role of ILCT transitions in controlling photophysical properties was evidenced for 76, 77, 79, 80, and 82.<sup>37,129–139</sup>

Comprehensive investigations of the mutual chromophore orientation on photophysical properties were performed for the pairs 78–79 and 82–83, in which the electronic coupling between the organic and metal-based chromophores were controlled by the anthryl linkage (78 and 79) and steric hindrance of the 4-(methyl)phenyl substituent introduced into the imidazole ring at 1H-position (82 and 83).

For complexes 78 and 83, with the high dihedral angle between the aryl substituent and diimine planes,  $\pi_{\text{arene}}-\pi_{\text{arene}}^*$  absorptions with characteristic vibronic progression are well resolved from the weak  $^1\text{MLCT}$  band occurring in the lower energy region. On contrary, compounds 79 and 82 with a more coplanar ligand geometry display the unstructured, noticeably red-shifted and more intense lowest energy absorption in comparison to 78 and 83 (Fig. 3). Such findings, that are red-shift and significant absorptivity enhancement, along with the lack of characteristic anthracene/pyrene vibronic progression, are





**Scheme 6**  $\text{Re}(\text{I})$  carbonyl complexes bearing diimine ligands substituted with electron-rich pyrenyl  $\pi$ -conjugated aryl groups.

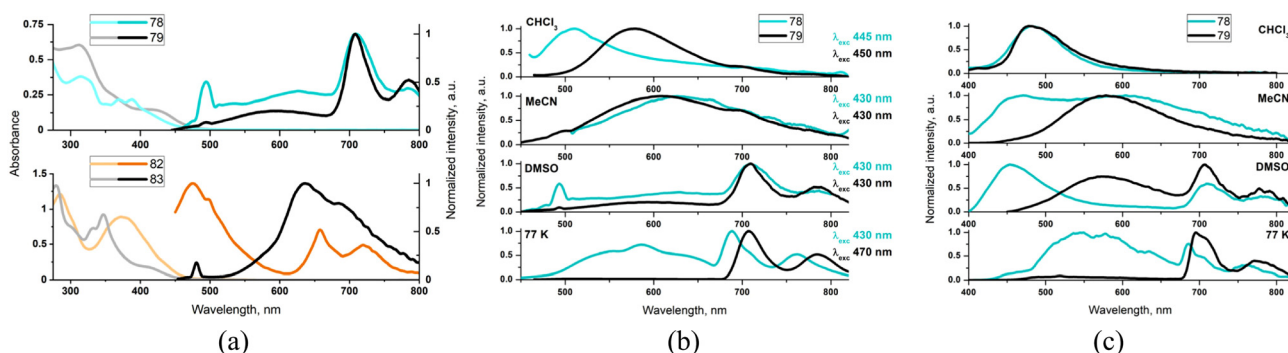


**Fig. 3** Photophysical data of 78–79 and 82–83: absorbance (lighter lines) and emission (darker lines) in DMSO (a); emission spectra of 78 and 79 in different environments upon excitation at the red side of the lowest energy absorption (b) and 355 nm (c). Adapted from ref. 136 and 137 Copyright © 2022, 2023, American Chemical Society.

strongly supportive of the contribution of intra-ligand charge transfer transitions from the electron-rich aryl group to the  $\pi$ -accepting diamine core.

The TA studies 78–79 and 82–83 revealed that a more planar ligand geometry in 78 and 82 facilitates the population of the long-lived triplet ligand-centered excited state. In

general, it is populated *via* the triplet-triplet energy transfer from  $^3\text{MLCT}$  excited state. For the complex **82**, the contribution of the another  $^1\text{ILpyrene}/^1\text{ILCT} \rightarrow ^3\text{ILpyrene}/^3\text{ILCT}$  pathway was also evidenced. Compared to **79** and **83**,  $\text{T}_1 \rightarrow \text{T}_n$  absorptions of **78** and **82** are noticeable red-shifted and broadening, in agreement with the contribution of the photoinduced charge transfer processes occurring from the electron-rich aryl group to the  $\pi$ -accepting diamine core. The lowest triplet excited state was found to be of  $^3\text{IL}_{\text{arene}}/^3\text{ILCT}$  for **79** and **82** and  $^3\text{IL}_{\text{arene}}$  for **78** and **83**. The complexes **78**, **79** and **83** were found to be rare examples of coordination compounds that show aryl-based phosphorescence in solution at RT. As demonstrated by steady-state emission studies, the population of  $^3\text{MLCT}$  and  $^3\text{IL}_{\text{arene}}$  of **78** and **79** can be controlled by the solvent polarity and excitation wavelengths (Fig. 3). In DMSO, compounds **78** and **79** upon excitations  $\lambda > 410$  nm show a dual  $^3\text{MLCT}$  and  $^3\text{An}$  emission, extremely rarely observed.

Having long excited-state lifetimes (Table S6†), the complexes **78–79** and **82–83** were found to be suitable for transferring the excited triplet-state energy to molecular oxygen and generating singlet oxygen. The pyrenyl-substituted complexes, with record-high triplet excited-state lifetimes at RT ( $\sim 1800$   $\mu\text{s}$  for **82** and  $\sim 1500$   $\mu\text{s}$  for **83**) act also as photosensitizers in triplet-triplet annihilation upconversion.<sup>136,137</sup> Using TA spectroscopy, the complex **80** was demonstrated to exhibit ‘ping-pong’ energy transfer  $^1\text{ILCT} \rightarrow ^1\text{MLCT} \rightarrow ^3\text{MLCT} \rightarrow ^3\text{IL}/^3\text{ILCT}$ . In agreement with the triplet-state equilibrium between  $^3\text{MLCT} \rightarrow ^3\text{IL}/^3\text{ILCT}$ , the complex **80** shows an extended triplet excited-state lifetime at RT (4.4  $\mu\text{s}$ ).<sup>135</sup> The combined spectroscopic data of **77** were found to be consistent with lowest triplet excited state being either of  $^3\text{IL}$  or  $^3\text{ILCT}$  character.<sup>129</sup>

Importantly, the incorporation of  $\pi$ -conjugated aryl groups into the diimine cores of Re(i) carbonyl complexes, which facilitates a population of the triplet ligand-centered excited state and enhances photoinduced energy transfer processes, were found to be a powerful strategy to design more efficient catalysts for the conversion of  $\text{CO}_2$  into CO using solar energy (see next section).

#### 4. Appealing applications of Re(i) complexes with D–A or D– $\pi$ –A diimine ligands

The rhodium(i) tricarbonyl complexes bearing  $\pi$ -extended pyrene and anthracene chromophores attached to the diimine ligand **73**, **76**, and **84** were garnered substantial attention for the light-driven  $\text{CO}_2$ -to-CO reduction.<sup>132–134</sup> The appended  $\pi$ -extended aryl groups were demonstrated to promote the Re(i) catalyst’s ability, which was rationalized by their increased visible light-harvesting abilities and long-lived excited states corresponding to the ligand-localized triplet state compared to the appropriate reference Re(i) complexes (see section 3.3). Most importantly, the complex **76** was the first example of a single-molecule catalyst investigated directly under the sun.

Relative to the model chromophore  $[\text{ReCl}(\text{CO})_3(\text{bipy})]$  ( $\text{TON}_{\text{CO}} = 22 \pm 2$ ), the turnover number  $\text{TON}_{\text{CO}}$  of the complex **76** was 40-fold higher ( $350 \pm 36$ ) under these conditions.<sup>133</sup>

The terpyridine-based complex  $[\text{ReCl}(\text{CO})_3(\text{Me}_2\text{N}-\text{C}_6\text{H}_4\text{-terpy-}\kappa^2\text{N})]$  (**52**) was the first Re(i) carbonyl system, which was tested as photosensitizer in the photocatalytic hydrogen production. Its  $^3\text{ILCT}$  excited-state reactivity was analysed relative to  $[\text{ReCl}(\text{CO})_3(\text{C}_6\text{H}_5\text{-terpy-}\kappa^2\text{N})]$ , possessing a much shorter-lived  $^3\text{MLCT}$  excited state. For  $[\text{ReCl}(\text{CO})_3(\text{Me}_2\text{N}-\text{C}_6\text{H}_4\text{-terpy-}\kappa^2\text{N})]$ , the hydrogen evolution was found to occur dramatically faster and with a noticeably higher final turnover number. Also, 10-fold-smaller concentration of  $[\text{ReCl}(\text{CO})_3(\text{Me}_2\text{N}-\text{C}_6\text{H}_4\text{-terpy-}\kappa^2\text{N})]$  was needed compared to the model chromophore. A striking difference between  $[\text{ReCl}(\text{CO})_3(\text{Me}_2\text{N}-\text{C}_6\text{H}_4\text{-terpy-}\kappa^2\text{N})]$  and  $[\text{ReCl}(\text{CO})_3(\text{C}_6\text{H}_5\text{-terpy-}\kappa^2\text{N})]$  was evidenced using TRIR spectroscopy. While  $[\text{ReCl}(\text{CO})_3(\text{Me}_2\text{N}-\text{C}_6\text{H}_4\text{-terpy-}\kappa^2\text{N})]$  was found to transfer the electron directly to the cobalt catalyst, the model chromophore underwent the reductive quenching in a bimolecular fashion by triethanolamine, used as the sacrificial donor.<sup>108</sup>

The terpyridine Re(i) complexes  $[\text{ReCl}(\text{CO})_3(\text{R-terpy-}\kappa^2\text{N})]$  with appended  $\pi$ -extended aryl and electron-donating amine groups (**52**, **78**, **80**) were also emerged as a novel category of anticancer agents. Possessing abilities for both  $^1\text{O}_2$  generation and releasing CO under ultrasound irradiation, they could be regarded as combined agents for photodynamic therapy and photo-activated chemotherapy.<sup>37,140</sup>

Last but not least, the Re(i) compounds bearing diimine ligand of D–A or D– $\pi$ –A type deserved an attention in view of their potential applications as phosphorescent emitting materials in OLED technology. Excellent device performances were achieved for OLEDs with Re(i) complexes **41–43** as dopant emitters. The last of them (**43**) showed the performance with a maximum current efficiency of 36.5 cd A $^{-1}$ , maximum power efficiency of 31.7 lm W $^{-1}$  and maximum external quantum efficiency of 12.0%, which were among the best data for the Re(i)-based OLEDs reported so far.<sup>3,5</sup>

#### 5. Summary and future prospects

The growth of many technologies, including photocatalysis, photodynamic therapy and triplet-triplet annihilation for energy up-conversion, requires efficient photosensitizers with strong absorption in the visible range, good solubility and sufficiently long excited state lifetimes. Within this review, we summarized the latest developments concerning the bichromophoric effect in diimine Re(i) tricarbonyls functionalized with electron-rich donors. It was demonstrated that the formation of intraligand charge transfer (ILCT) excited states, due to incorporation of the organic push-pull chromophore to the  $\{\text{Re}(\text{CO})_3\}^+$  core, may lead to enhancement of visible absorptivity, bathochromic shift of the emission and significant prolongation of the excited-state lifetimes of these systems. The role of ILCT transitions in controlling of excited state properties was discussed for Re(i) tricarbonyls bearing six



different diimine cores (bipy, terpy, phen, dppz, imphen, pybimd and pytri), decorated by various electron-rich amine, sulphur-based and  $\pi$ -conjugated aryl groups.

Although a huge progress has been made in understanding photoinduced processes occurring in bichromophoric Re(i) complexes bearing donor–acceptor ligands, a precise control of long-lived charge-separated excited states in these systems still remains a major challenge, and more advanced studies in this field are strongly desired to establish structure–property relationships and make further progress in the development of more efficient materials. The current review clearly highlights that Re(i) complexes with imphen-, pybimd- and pytri-based ligands of the donor–acceptor structure is noticeably underdeveloped compared to those bearing derivatives of bipy, terpy, phen and dppz. In particular, the research with the use of highly advanced and time-resolved spectroscopic measurement techniques are most required to provide a more complete picture of excited state dynamics and rate of formation of triplet excited states in these systems. Regarding a type of a donor part, Re(i) tricarbonyl complexes with diimines bearing sulphur-based electron-rich groups deserves more scientific attention, especially that the Ru(ii) complex with terthiophene-substituted imidazo[4,5-f][1,10]phenanthroline (TLD1433)<sup>64</sup> is the first organometallic photosensitizers introduced into a human clinical trial, and Re(i) tricarbonyls bearing imphen-based ligands have recently emerged as promising anticancer agents.<sup>117,141</sup> An important advantage of imidazo[4,5-f][1,10]phenanthrolines is their convenient synthesis along with the possibility of introduction all types of into the imidazole ring at 1H- and C2-positions, directly (*via* the covalent bond) or through an aryl/heterocycle bridge, giving the possibility to establish reliable structure–property relationships. Furthermore, as demonstrated in section 3.3, the mutual chromophore arrangement in  $[\text{ReL}(\text{CO})_3(\text{R}^1\text{R}^2\text{-imphen})]^n$  with  $\pi$ -conjugated aryl groups, controlled by steric hindrance of the substituent introduced into the imidazole ring at 1H-position, impacts the efficiency of intermolecular photoinduced energy triplet state transfers. Explorations of spatial effects in these systems seem to be interesting future research direction. Regarding Re(i) tricarbonyl complexes with bipy- and phen-based ligands of the donor–acceptor structure, a research gap concerns investigations of the effect of different ligand substitution patterns. The introduction of donor groups into different positions of 2,2'-bipyridine and 1,10-phenanthroline skeleton is expected to provide different electron density delocalization, which may be essential in controlling photoinduced charge-transfer processes. Finally, to facilitate population of ILCT excited states, a scientific attention should be directed towards Re(i) complexes with well-separated  $^1\text{ILCT}$  and  $^1\text{MLCT}$  absorption bands. Photo-induced charge-transfer processes in such systems could be precisely controlled by the excitation wavelength.

## Author contributions

The manuscript was written through the contributions of all authors. KC: formal analysis, visualization, writing – original

draft. JPG: data curation, writing – review & editing. AK: formal analysis, visualization. EM: project administration, supervision, validation. BM: conceptualization, funding acquisition, project administration, supervision, writing – original draft, writing – review & editing. All authors have given approval to the final version of the manuscript.

## Data availability

No primary research results, software or code have been included and no new data were generated or analysed as part of this review.

## Conflicts of interest

The authors declare no competing financial interest.

## Acknowledgements

This work was financed by the Research Excellence Initiative of the University of Silesia in Katowice.

## References

- 1 M. Wrighton and D. L. Morse, *J. Am. Chem. Soc.*, 1974, **96**, 998–1003.
- 2 R. C. Evans, P. Douglas and C. J. Winscom, *Coord. Chem. Rev.*, 2006, **250**, 2093–2126.
- 3 G.-W. Zhao, J.-H. Zhao, Y.-X. Hu, D.-Y. Zhang and X. Li, *Synth. Met.*, 2016, **212**, 131–141.
- 4 Y.-X. Hu, G.-W. Zhao, Y. Dong, Y.-L. Lü, X. Li and D.-Y. Zhang, *Dyes Pigm.*, 2017, **137**, 569–575.
- 5 X. Li, G.-W. Zhao, Y.-X. Hu, J.-H. Zhao, Y. Dong, L. Zhou, Y.-L. Lv, H.-J. Chi and Z. Su, *J. Mater. Chem. C*, 2017, **5**, 7629–7636.
- 6 M. R. Gonçalves, A. R. V. Benvenho and K. P. M. Frin, *Opt. Mater.*, 2019, **94**, 206–212.
- 7 C. Bizzarri, F. Hundemer, J. Busch and S. Bräse, *Polyhedron*, 2018, **140**, 51–66.
- 8 S. Gazzari, P. Dreyse, D. Cortés-Ariagada and I. A. González, *Mater. Sci. Semicond. Process.*, 2022, **147**, 106733.
- 9 H. Takeda and O. Ishitani, *Coord. Chem. Rev.*, 2010, **254**, 346–354.
- 10 J. Agarwal, E. Fujita, H. F. I. Schaefer and J. T. Muckerman, *J. Am. Chem. Soc.*, 2012, **134**, 5180–5186.
- 11 A. Zarkadoulas, E. Koutsouri, C. Kefalidi and C. A. Mitsopoulou, *Coord. Chem. Rev.*, 2015, **304–305**, 55–72.
- 12 Y. Yamazaki, H. Takeda and O. Ishitani, *J. Photochem. Photobiol. C*, 2015, **25**, 106–137.
- 13 N. Elgrishi, M. B. Chambers, X. Wang and M. Fontecave, *Chem. Soc. Rev.*, 2017, **46**, 761–796.



14 K. M. Choi, D. Kim, B. Rungtaweevoranit, C. A. Trickett, J. T. D. Barmanbek, A. S. Alshammari, P. Yang and O. M. Yaghi, *J. Am. Chem. Soc.*, 2017, **139**, 356–362.

15 L.-Q. Qiu, Z.-W. Yang, X. Yao, X.-Y. Li and L.-N. He, *ChemSusChem*, 2022, **15**, e202200337.

16 L. Wang, *Catalysts*, 2022, **12**, 919.

17 N. Nandal and S. L. Jain, *Coord. Chem. Rev.*, 2022, **451**, 214271.

18 A. V. Müller, L. A. Faustino, K. T. de Oliveira, A. O. T. Patrocínio and A. S. Polo, *ACS Catal.*, 2023, **13**, 633–646.

19 S. Hostachy, C. Policar and N. Delsuc, *Coord. Chem. Rev.*, 2017, **351**, 172–188.

20 L. C.-C. Lee, K.-K. Leung and K. K.-W. Lo, *Dalton Trans.*, 2017, **46**, 16357–16380.

21 C. C. Konkankit, S. C. Marker, K. M. Knopf and J. J. Wilson, *Dalton Trans.*, 2018, **47**, 9934–9974.

22 E. B. Bauer, A. A. Haase, R. M. Reich, D. C. Crans and F. E. Kühn, *Coord. Chem. Rev.*, 2019, **393**, 79–117.

23 P. Collery, D. Desmaele and V. Vijaykumar, *Curr. Pharm. Des.*, 2019, **25**, 3306–3322.

24 L. K. McKenzie, H. E. Bryant and J. A. Weinstein, *Coord. Chem. Rev.*, 2019, **379**, 2–29.

25 H. S. Liew, C.-W. Mai, M. Zulkefeli, T. Madheswaran, L. V. Kiew, N. Delsuc and M. L. Low, *Molecules*, 2020, **25**, 4176.

26 K. Schindler and F. Zobi, *Chimia*, 2021, **75**, 837–837.

27 C.-P. Tan, Y.-M. Zhong, L.-N. Ji and Z.-W. Mao, *Chem. Sci.*, 2021, **12**, 2357–2367.

28 J. Gong and X. Zhang, *Coord. Chem. Rev.*, 2022, **453**, 214329.

29 S. Pete, N. Roy, B. Kar and P. Paira, *Coord. Chem. Rev.*, 2022, **460**, 214462.

30 K. Schindler and F. Zobi, *Molecules*, 2022, **27**, 539.

31 A. Sharma S., N. Vaibhavi, B. Kar, U. Das and P. Paira, *RSC Adv.*, 2022, **12**, 20264–20295.

32 L. E. Enslin, K. Purkait, M. D. Pozza, B. Saubamea, P. Mesdom, H. G. Visser, G. Gasser and M. Schutte-Smith, *Inorg. Chem.*, 2023, **62**, 12237–12251.

33 B. Kar, U. Das, N. Roy and P. Paira, *Coord. Chem. Rev.*, 2023, **474**, 214860.

34 C. Olelewe and S. G. Awuah, *Curr. Opin. Chem. Biol.*, 2023, **72**, 102235.

35 Q. Qi, Q. Wang, Y. Li, D. Z. Silva, M. E. L. Ruiz, R. Ouyang, B. Liu and Y. Miao, *Molecules*, 2023, **28**, 2733.

36 K. Schindler, J. Horner, G. Demirci, Y. Cortat, A. Crochet, O. Mamula Steiner and F. Zobi, *Inorganics*, 2023, **11**, 139.

37 R. Kushwaha, A. Upadhyay, S. Saha, A. K. Yadav, A. Bera, A. Dutta and S. Banerjee, *Dalton Trans.*, 2024, **53**, 13591–13601.

38 R. Kushwaha, V. Singh, S. Peters, A. K. Yadav, T. Sadhukhan, B. Koch and S. Banerjee, *J. Med. Chem.*, 2024, **67**, 6537–6548.

39 A. Marco, P. Ashoo, S. Hernández-García, P. Martínez-Rodríguez, N. Cutillas, A. Vollrath, D. Jordan, C. Janiak, F. Gandía-Herrero and J. Ruiz, *J. Med. Chem.*, 2024, **67**, 7891–7910.

40 T. Neumann, V. Ramu, J. Bertin, M. He, C. Vervisch, M. P. Coogan and H. C. Bertrand, *Inorg. Chem.*, 2024, **63**, 1197–1213.

41 M. W. George and J. J. Turner, *Coord. Chem. Rev.*, 1998, **177**, 201–217.

42 A. Vlček and M. Busby, *Coord. Chem. Rev.*, 2006, **250**, 1755–1762.

43 A. Cannizzo, A. M. Blanco-Rodríguez, A. El Nahhas, J. Šebera, S. Záliš, A. Vlček Jr. and M. Chergui, *J. Am. Chem. Soc.*, 2008, **130**, 8967–8974.

44 M. K. Kuimova, W. Z. Alsindi, A. J. Blake, E. S. Davies, D. J. Lampus, P. Matousek, J. McMaster, A. W. Parker, M. Towrie, X.-Z. Sun, C. Wilson and M. W. George, *Inorg. Chem.*, 2008, **47**, 9857–9869.

45 A. El Nahhas, A. Cannizzo, F. van Mourik, A. M. Blanco-Rodríguez, S. Záliš, A. Vlček Jr. and M. Chergui, *J. Phys. Chem. A*, 2010, **114**, 6361–6369.

46 A. Vlček, in *Photophysics of Organometallics*, ed. A. J. Lees, Springer, Berlin, Heidelberg, 2010, pp. 115–158.

47 A. El Nahhas, C. Consani, A. M. Blanco-Rodríguez, K. M. Lancaster, O. Braem, A. Cannizzo, M. Towrie, I. P. Clark, S. Záliš, M. Chergui and A. Vlček, *Inorg. Chem.*, 2011, **50**, 2932–2943.

48 Y. Yue, T. Grusenmeyer, Z. Ma, P. Zhang, T. T. Pham, J. T. Mague, J. P. Donahue, R. H. Schmehl, D. N. Beratan and I. V. Rubtsov, *J. Phys. Chem. B*, 2013, **117**, 15903–15916.

49 L. M. Kiefer, J. T. King and K. J. Kubarych, *Acc. Chem. Res.*, 2015, **48**, 1123–1130.

50 R. Horvath, G. S. Huff, K. C. Gordon and M. W. George, *Coord. Chem. Rev.*, 2016, **325**, 41–58.

51 K. Choroba, S. Kotowicz, A. Maroń, A. Świtlicka, A. Szlapa-Kula, M. Siwy, J. Grzelak, K. Sulowska, S. Maćkowski, E. Schab-Balcerzak and B. Machura, *Dyes Pigm.*, 2021, **192**, 109472.

52 A. Szlapa-Kula, J. Palion-Gazda, P. Ledwon, K. Erfurt and B. Machura, *Dalton Trans.*, 2022, **51**, 14466–14481.

53 D. R. Striplin and G. A. Crosby, *Coord. Chem. Rev.*, 2001, **211**, 163–175.

54 A. M. Blanco Rodríguez, A. Gabrielsson, M. Motevalli, P. Matousek, M. Towrie, J. Šebera, S. Záliš and A. Vlček, *J. Phys. Chem. A*, 2005, **109**, 5016–5025.

55 A. Vlček and S. Záliš, *Coord. Chem. Rev.*, 2007, **251**, 258–287.

56 A. Coleman, C. Brennan, J. G. Vos and M. T. Pryce, *Coord. Chem. Rev.*, 2008, **252**, 2585–2595.

57 A. Kumar, S.-S. Sun and A. J. Lees, in *Photophysics of Organometallics*, ed. A. J. Lees, Springer, Berlin, Heidelberg, 2010, pp. 37–71.

58 R. Baková, M. Chergui, C. Daniel, A. Vlček and S. Záliš, *Coord. Chem. Rev.*, 2011, **255**, 975–989.

59 C. Daniel, *Coord. Chem. Rev.*, 2015, **282–283**, 19–32.

60 J. R. Dilworth, *Coord. Chem. Rev.*, 2021, **436**, 213822.



61 Z. R. Grabowski, K. Rotkiewicz and W. Rettig, *Chem. Rev.*, 2003, **103**, 3899–4032.

62 R. Misra and S. P. Bhattacharyya, in *Intramolecular Charge Transfer*, ed. R. Misra and S. P. Bhattacharyya, 2018, pp. 115–148.

63 A. Ito, M. Iwamura and E. Sakuda, *Coord. Chem. Rev.*, 2022, **467**, 214610.

64 S. Monro, K. L. Colón, H. Yin, J. Roque, P. Konda, S. Gujar, R. P. Thummel, L. Lilge, C. G. Cameron and S. A. McFarland, *Chem. Rev.*, 2019, **119**, 797–828.

65 T. C. Pham, V.-N. Nguyen, Y. Choi, S. Lee and J. Yoon, *Chem. Rev.*, 2021, **121**, 13454–13619.

66 K. Y. Zhang, Q. Yu, H. Wei, S. Liu, Q. Zhao and W. Huang, *Chem. Rev.*, 2018, **118**, 1770–1839.

67 J. Zhou, Q. Liu, W. Feng, Y. Sun and F. Li, *Chem. Rev.*, 2015, **115**, 395–465.

68 W. Ahmad, J. Wang, H. Li, Q. Ouyang, W. Wu and Q. Chen, *Coord. Chem. Rev.*, 2021, **439**, 213944.

69 R. Pérez-Ruiz, *Top. Curr. Chem.*, 2022, **380**, 23.

70 G. S. Huff, W. K. C. Lo, R. Horvath, J. O. Turner, X.-Z. Sun, G. R. Weal, H. J. Davidson, A. D. W. Kennedy, C. J. McAdam, J. D. Crowley, M. W. George and K. C. Gordon, *Inorg. Chem.*, 2016, **55**, 12238–12253.

71 M. G. Fraser, A. G. Blackman, G. I. S. Irwin, C. P. Easton and K. C. Gordon, *Inorg. Chem.*, 2010, **49**, 5180–5189.

72 M. R. Waterland, K. C. Gordon, J. J. McGarvey and P. M. Jayaweera, *J. Chem. Soc., Dalton Trans.*, 1998, 609–616.

73 M. I. J. Polson, S. L. Howell, A. H. Flood, A. K. Burrell, A. G. Blackman and K. C. Gordon, *Polyhedron*, 2004, **23**, 1427–1439.

74 B. D. Rossenaar, D. J. Stufkens and A. Vlček, *Inorg. Chem.*, 1996, **35**, 2902–2909.

75 D. J. Liard, M. Busby, P. Matousek, M. Towrie and A. Vlček, *J. Phys. Chem. A*, 2004, **108**, 2363–2369.

76 M. Chergui, *Acc. Chem. Res.*, 2015, **48**, 801–808.

77 M. K. Kuimova, D. C. Grills, P. Matousek, A. W. Parker, X.-Z. Sun, M. Towrie and M. W. George, *Vib. Spectrosc.*, 2004, **35**, 219–223.

78 K. Wang, L. Huang, L. Gao, L. Jin and C. Huang, *Inorg. Chem.*, 2002, **41**, 3353–3358.

79 R. Czerwieniec, A. Kapturkiewicz, J. Lipkowski and J. Nowacki, *Inorg. Chim. Acta*, 2005, **358**, 2701–2710.

80 T. Y. Kim, A. B. S. Elliott, K. J. Shaffer, C. John McAdam, K. C. Gordon and J. D. Crowley, *Polyhedron*, 2013, **52**, 1391–1398.

81 W. K. C. Lo, G. S. Huff, J. R. Cubanski, A. D. W. Kennedy, C. J. McAdam, D. A. McMorran, K. C. Gordon and J. D. Crowley, *Inorg. Chem.*, 2015, **54**, 1572–1587.

82 S. Sinha, E. K. Berdichevsky and J. J. Warren, *Inorg. Chim. Acta*, 2017, **460**, 63–68.

83 A. M. Mansour, *RSC Adv.*, 2019, **9**, 15108–15114.

84 J. Palion-Gazda, K. Choroba, A. M. Maroń, E. Malicka and B. Machura, *Molecules*, 2024, **29**, 1631.

85 J. Palion-Gazda, K. Choroba, M. Penkala, P. Rawicka and B. Machura, *Inorg. Chem.*, 2024, **63**, 1356–1366.

86 O. D. C. C. De Azevedo, P. I. P. Elliott, C. D. Gabbett, B. M. Heron, D. Jacquemin, C. R. Rice and P. A. Scattergood, *Dalton Trans.*, 2021, **50**, 830–834.

87 B.-C. Tzeng, B.-S. Chen, C.-K. Chen, Y.-P. Chang, W.-C. Tzeng, T.-Y. Lin, G.-H. Lee, P.-T. Chou, Y.-J. Fu and A. H.-H. Chang, *Inorg. Chem.*, 2011, **50**, 5379–5388.

88 M. Obata, A. Kitamura, A. Mori, C. Kameyama, J. A. Czaplewska, R. Tanaka, I. Kinoshita, T. Kusumoto, H. Hashimoto, M. Harada, Y. Mikata, T. Funabiki and S. Yano, *Dalton Trans.*, 2008, 3292–3300.

89 J. R. Schoonover, W. D. Bates and T. J. Meyer, *Inorg. Chem.*, 1995, **34**, 6421–6422.

90 Y. Kim, F. W. M. Vanhelmont, C. L. Stern and J. T. Hupp, *Inorg. Chim. Acta*, 2001, **318**, 53–60.

91 C. Liu, J. Li, B. Li, Z. Hong, F. Zhao, S. Liu and W. Li, *Appl. Phys. Lett.*, 2006, **89**, 243511.

92 C. B. Liu, J. Li, B. Li, Z. R. Hong, F. F. Zhao, S. Y. Liu and W. L. Li, *Chem. Phys. Lett.*, 2007, **435**, 54–58.

93 R. Horvath, M. G. Fraser, S. A. Cameron, A. G. Blackman, P. Wagner, D. L. Officer and K. C. Gordon, *Inorg. Chem.*, 2013, **52**, 1304–1317.

94 T. Yu, D. P.-K. Tsang, V. K.-M. Au, W. H. Lam, M.-Y. Chan and V. W.-W. Yam, *Chem. – Eur. J.*, 2013, **19**, 13418–13427.

95 C. B. Larsen, H. van der Salm, C. A. Clark, A. B. S. Elliott, M. G. Fraser, R. Horvath, N. T. Lucas, X.-Z. Sun, M. W. George and K. C. Gordon, *Inorg. Chem.*, 2014, **53**, 1339–1354.

96 H. van der Salm, C. B. Larsen, J. R. W. McLay, G. S. Huff and K. C. Gordon, *Inorg. Chim. Acta*, 2015, **428**, 1–7.

97 C. B. Larsen, H. van der Salm, G. E. Shillito, N. T. Lucas and K. C. Gordon, *Inorg. Chem.*, 2016, **55**, 8446–8458.

98 B. S. Adams, G. E. Shillito, H. van der Salm, R. Horvath, C. B. Larsen, X.-Z. Sun, N. T. Lucas, M. W. George and K. C. Gordon, *Inorg. Chem.*, 2017, **56**, 12967–12977.

99 G. E. Shillito, T. B. J. Hall, D. Preston, P. Traber, L. Wu, K. E. A. Reynolds, R. Horvath, X. Z. Sun, N. T. Lucas, J. D. Crowley, M. W. George, S. Kupfer and K. C. Gordon, *J. Am. Chem. Soc.*, 2018, **140**, 4534–4542.

100 J. E. Barnsley, G. E. Shillito, C. B. Larsen, H. van der Salm, R. Horvath, X. Z. Sun, X. Wu, M. W. George, N. T. Lucas and K. C. Gordon, *Inorg. Chem.*, 2019, **58**, 9785–9795.

101 T. Klemens, A. Świtlicka, A. Szlapa-Kula, Ł. Łapok, M. Obłoza, M. Siwy, M. Szalkowski, S. Maćkowski, M. Libera, E. Schab-Balcerzak and B. Machura, *Organometallics*, 2019, **38**, 4206–4223.

102 G. E. Shillito, D. Preston, P. Traber, J. Steinmetzer, C. J. McAdam, J. D. Crowley, P. Wagner, S. Kupfer and K. C. Gordon, *Inorg. Chem.*, 2020, **59**, 6736–6746.

103 D. A. W. Ross, J. I. Mapley, A. P. Cording, R. A. S. Vasdev, C. J. McAdam, K. C. Gordon and J. D. Crowley, *Inorg. Chem.*, 2021, **60**, 11852–11865.

104 J. J. Sutton, D. Preston, P. Traber, J. Steinmetzer, X. Wu, S. Kayal, X.-Z. Sun, J. D. Crowley, M. W. George, S. Kupfer and K. C. Gordon, *J. Am. Chem. Soc.*, 2021, **143**, 9082–9093.



105 G. E. Shillito, D. Preston, J. D. Crowley, P. Wagner, S. J. Harris, K. C. Gordon and S. Kupfer, *Inorg. Chem.*, 2024, **63**, 4947–4956.

106 A. M. Maroń, A. Szlapa-Kula, M. Matussek, R. Kruszynski, M. Siwy, H. Janeczek, J. Grzelak, S. Maćkowski, E. Schab-Balcerzak and B. Machura, *Dalton Trans.*, 2020, **49**, 4441–4453.

107 T. Klemens, A. Świtlicka-Olszewska, B. Machura, M. Grucela, H. Janeczek, E. Schab-Balcerzak, A. Szlapa, S. Kula, S. Krompiec, K. Smolarek, D. Kowalska, S. Mackowski, K. Erfurt and P. Lodziński, *RSC Adv.*, 2016, **6**, 56335–56352.

108 R. Fernández-Terán and L. Sévery, *Inorg. Chem.*, 2021, **60**, 1334–1343.

109 J. Palion-Gazda, A. Szlapa-Kula, M. Penkala, K. Erfurt and B. Machura, *Molecules*, 2022, **27**, 7147.

110 T. Klemens, A. Świtlicka, A. Szlapa-Kula, S. Krompiec, P. Lodziński, A. Chrobok, M. Godlewska, S. Kotowicz, M. Siwy, K. Bednarczyk, M. Libera, S. Maćkowski, T. Pędziński, E. Schab-Balcerzak and B. Machura, *Appl. Organomet. Chem.*, 2018, **32**, e4611.

111 K. Choroba, A. Maroń, A. Świtlicka, A. Szlapa-Kula, M. Siwy, J. Grzelak, S. Maćkowski, T. Pędziński, E. Schab-Balcerzak and B. Machura, *Dalton Trans.*, 2021, **50**, 3943–3958.

112 D. Hanss and O. S. Wenger, *Inorg. Chim. Acta*, 2009, **362**, 3415–3420.

113 J.-X. Wang, H.-Y. Xia, W.-Q. Liu, F. Zhao and Y. Wang, *Inorg. Chim. Acta*, 2013, **394**, 92–97.

114 T. Klemens, A. Świtlicka-Olszewska, B. Machura, M. Grucela, E. Schab-Balcerzak, K. Smolarek, S. Mackowski, A. Szlapa, S. Kula, S. Krompiec, P. Lodziński and A. Chrobok, *Dalton Trans.*, 2016, **45**, 1746–1762.

115 J. R. W. McLay, J. J. Sutton, G. E. Shillito, C. B. Larsen, G. S. Huff, N. T. Lucas and K. C. Gordon, *Inorg. Chem.*, 2021, **60**, 130–139.

116 E. J. Rohwer, Y. Geng, M. Akbarimoosavi, L. M. L. Daku, O. Aleveque, E. Levillain, J. Hauser, A. Cannizzo, R. Häner, S. Decurtins, R. J. Stanley, T. Feurer and S.-X. Liu, *Chem. – Eur. J.*, 2021, **27**, 5399–5403.

117 X. Su, W.-J. Wang, Q. Cao, H. Zhang, B. Liu, Y. Ling, X. Zhou and Z.-W. Mao, *Angew. Chem., Int. Ed.*, 2022, **61**, e202115800.

118 Y.-Q. Li and K.-Z. Wang, *Molecules*, 2023, **28**, 3229.

119 W. E. Ford and M. A. J. Rodgers, *J. Phys. Chem.*, 1992, **96**, 2917–2920.

120 N. D. McClenaghan, Y. Leydet, B. Maubert, M. T. Indelli and S. Campagna, *Coord. Chem. Rev.*, 2005, **249**, 1336–1350.

121 J. Zhao, W. Wu, J. Sun and S. Guo, *Chem. Soc. Rev.*, 2013, **42**, 5323–5351.

122 X. Cui, J. Zhao, Z. Mohmood and C. Zhang, *Chem. Rec.*, 2016, **16**, 173–188.

123 X. Zhang, Y. Hou, X. Xiao, X. Chen, M. Hu, X. Geng, Z. Wang and J. Zhao, *Coord. Chem. Rev.*, 2020, **417**, 213371.

124 X. Zhao, Y. Hou, L. Liu and J. Zhao, *Energy Fuels*, 2021, **35**, 18942–18956.

125 I. E. Pomestchenko, C. R. Luman, M. Hissler, R. Ziessel and F. N. Castellano, *Inorg. Chem.*, 2003, **42**, 1394–1396.

126 S. Ji, W. Wu, W. Wu, P. Song, K. Han, Z. Wang, S. Liu, H. Guo and J. Zhao, *J. Mater. Chem.*, 2010, **20**, 1953–1963.

127 W. Wu, J. Sun, S. Ji, W. Wu, J. Zhao and H. Guo, *Dalton Trans.*, 2011, **40**, 11550–11561.

128 Q. Li, H. Guo, L. Ma, W. Wu, Y. Liu and J. Zhao, *J. Mater. Chem.*, 2012, **22**, 5319–5329.

129 A. Del Guerzo, S. Leroy, F. Fages and R. H. Schmehl, *Inorg. Chem.*, 2002, **41**, 359–366.

130 N. M. Shavaleev, Z. R. Bell, T. L. Easun, R. Rutkaite, L. Swanson and M. D. Ward, *Dalton Trans.*, 2004, 3678–3688.

131 M. E. Walther and O. S. Wenger, *Dalton Trans.*, 2008, 6311–6318.

132 N. P. Liyanage, W. Yang, S. Guertin, S. S. Roy, C. A. Carpenter, R. E. Adams, R. H. Schmehl, J. H. Delcamp and J. W. Jurss, *Chem. Commun.*, 2019, **55**, 993–996.

133 L.-Q. Qiu, K.-H. Chen, Z.-W. Yang and L.-N. He, *Green Chem.*, 2020, **22**, 8614–8622.

134 L.-Q. Qiu, K.-H. Chen, Z.-W. Yang, F.-Y. Ren and L.-N. He, *Chem. – Eur. J.*, 2021, **27**, 15536–15544.

135 A. Szlapa-Kula, M. Małecka, A. M. Maroń, H. Janeczek, M. Siwy, E. Schab-Balcerzak, M. Szalkowski, S. Maćkowski, T. Pędziński, K. Erfurt and B. Machura, *Inorg. Chem.*, 2021, **60**, 18726–18738.

136 M. Małecka, A. Szlapa-Kula, A. M. Maroń, P. Ledwon, M. Siwy, E. Schab-Balcerzak, K. Sulowska, S. Maćkowski, K. Erfurt and B. Machura, *Inorg. Chem.*, 2022, **61**, 15070–15084.

137 K. Choroba, M. Penkala, J. Palion-Gazda, E. Malicka and B. Machura, *Inorg. Chem.*, 2023, **62**, 19256–19269.

138 R. Das and P. Paira, *Dalton Trans.*, 2023, **52**, 15365–15376.

139 L. T. Babu, U. Das, R. Das, B. Kar and P. Paira, *Dalton Trans.*, 2024, **53**, 5993–6005.

140 Y. Li, N. Lu, Q. Lin, H. Wang, Z. Liang, Y. Lu and P. Zhang, *Chin. Chem. Lett.*, 2023, **34**, 107653.

141 K. S. Kisel, J. R. Shakirova, V. V. Pavlovskiy, R. A. Evarestov, V. V. Gurzhiy and S. P. Tunik, *Inorg. Chem.*, 2023, **62**, 18625–18640.

